

# A quasi-one-dimensional unsteady laminar flame formulation with independent strain rate and curvature

Raymond L. Speth<sup>a</sup>, Youssef M. Marzouk<sup>b</sup>, Ahmed F. Ghoniem<sup>a,\*</sup>

<sup>a</sup>Massachusetts Institute of Technology, 77 Massachusetts Avenue, Cambridge, MA 02139, USA

<sup>b</sup>Sandia National Laboratories, Livermore, CA 94551, USA

---

## Abstract

We present a new formulation of a cylindrical laminar flame in which unsteady strain rate and curvature are explicit, independent parameters. The formulation is described by a one-dimensional set of governing equations incorporating detailed kinetics and transport. We demonstrate the impact of curvature on the structure of strained premixed methane–air flames.

*Keywords:* Turbulent combustion; Laminar flames; Flame curvature; Flame stretch; Potential flow

---

## 1. Introduction

The impact of strain rate and curvature on flame structure and propagation is fundamental to the dynamics of turbulent combustion. Numerous theoretical [1] and computational [2] studies have sought to correlate flame speed with flame stretch  $\kappa$ , defined as the fractional rate-of-change of flame surface area:

$$\kappa \equiv \frac{1}{\delta A} \frac{d\delta A}{dt} = a + S_d \nabla \cdot \mathbf{n} \quad (1)$$

where  $\mathbf{n}$  is the flame unit normal vector, pointing towards the unburned mixture,  $S_d$  is the propagation speed of the flame relative to the unburned mixture,  $a = \nabla_T \cdot \mathbf{u}$  is the tangential strain rate, and  $\nabla \cdot \mathbf{n}$  is the curvature. While strain rate and curvature both contribute to stretch, each affects the convection–diffusion–reaction balance within the flame through different mechanisms. Thus, a simple correlation of flame stretch  $\kappa$  with burning velocity, while a useful theoretical tool, breaks down under realistic conditions of turbulent combustion: detailed kinetics and transport, high strain rates and curvatures, and unsteadiness in both of the latter. The strain rate history is crucial to predicting the burning rate of a flame element, for instance [3,4]; the response of a flame to the surrounding flow field depends on internal timescales. As with strain rate, the

impact of curvature on flame structure is tightly coupled to the transport properties of participating species – in particular, non-unity Lewis number effects and differential diffusion. For example, light species such as H may be ‘focused’ ahead of the flame in regions of negative curvature [5], enhancing the local burning rate.

The effects of curvature have been the subject of several recent studies, ranging from experimental studies of laminar flames [6] to two-dimensional direct simulations [5], but these studies have not been formulated in a way that generically separates the effects of strain rate and curvature. Typically, strain rate and curvature are implicit properties of the model that are analyzed in post-processing.

Quasi-one-dimensional flame models have strong relevance to the preceding discussion. In the flamelet regime of turbulent combustion, the flame surface is modeled as an ensemble of locally one-dimensional flames that respond instantaneously to the local strain rate. Unsteady Lagrangian approaches, such as the flame embedding model developed in [3], relax some of these idealizations and take into account the history of each flame element, thus capturing a range of unsteady flow–flame interactions. Flame structure and burning rate predictions with these models have been quite successful, but the effects of curvature have thus far been neglected.

This paper presents a new quasi-one-dimensional flame formulation in which curvature and strain rate are explicit, independent parameters of the model. The

---

\* Corresponding author. Tel.: +1 (617) 253 2295, Fax: +1 (617) 253 5981; E-mail: ghoniem@mit.edu

formulation is fully unsteady and incorporates detailed kinetics and transport. Using this computational tool, we seek a fundamental understanding of the mechanisms by which strain rate and curvature – both steady and unsteady – affect flame structure and burning. We also expect the model to advance the state of the art in subgrid models for multi-dimensional reacting flow.

## 2. Model formulation

### 2.1. Geometry

To develop a model of a curved flame, we consider a flame strained in an axisymmetric stagnation point flow. The simplest such potential flow is a uniform radial inflow with the stagnation point at  $r = 0$ . The velocity field is  $u = a(t)z$  and  $v = -\frac{1}{2}a(t)r$ , where  $u$  and  $v$  are the velocities in the axial ( $z$ ) and radial ( $r$ ) directions, respectively, and  $a(t)$  is a time-varying strain rate parameter. By adding a line source of flow along the axis  $r = 0$ , the stagnation plane becomes a cylinder at a finite radius  $R$  determined by the magnitude of the source. The corresponding velocity field is:

$$v = \frac{a}{2} \left( \frac{R^2 - r^2}{r} \right); \quad u = az \quad (2)$$

A cylindrical premixed flame may be established with this velocity field as the outer, non-reacting flow by making the mixture emanating from  $r = 0$  consist of reactants and the mixture from  $r = \infty$  consist of combustion products. The radial coordinate  $r$  is normal to the flame surface.

In the steady case, the cylindrical flame will typically rest on the inside of the stagnation surface; flame propagation in the negative radial direction is balanced by the local flow velocity. This is a negatively curved flame, convex toward the burned gas. The reverse configuration may also be considered, with products coming from the centerline and reactants coming from infinity. This is a positively curved flame, concave toward the burned gas, propagating in the positive radial direction. These flame configurations are illustrated in Fig. 1. We emphasize that this formulation admits two parameters for describing the outer flow: the strain rate parameter  $a(t)$  and the stagnation plane radius  $R$ .

### 2.2. Governing equations

Governing equations for the curved premixed flame are based on equations for reacting flow in cylindrical coordinates given by Kee [7]. The equations are simplified by neglecting viscous dissipation, thermal radiation, and by using a low-Mach-number assumption. We apply a boundary layer approximation across the flame and consider a solution along the stagnation streamline  $z = 0$ . The outer potential flow in Eq. (2) yields the axial pressure gradient:

$$\frac{\partial p}{\partial z} = -\rho z a^2 - \rho z \frac{da}{dt} \quad (3)$$

The unburned mixture density is  $\rho_{ub}$  and the axial velocity of the unburned mixture is  $u_{ub}$ . Introducing the similarity variable  $U \equiv u/u_{ub}$  and the notation  $V \equiv \rho v$ , and substituting the pressure gradient into the equation for momentum conservation inside the boundary layer

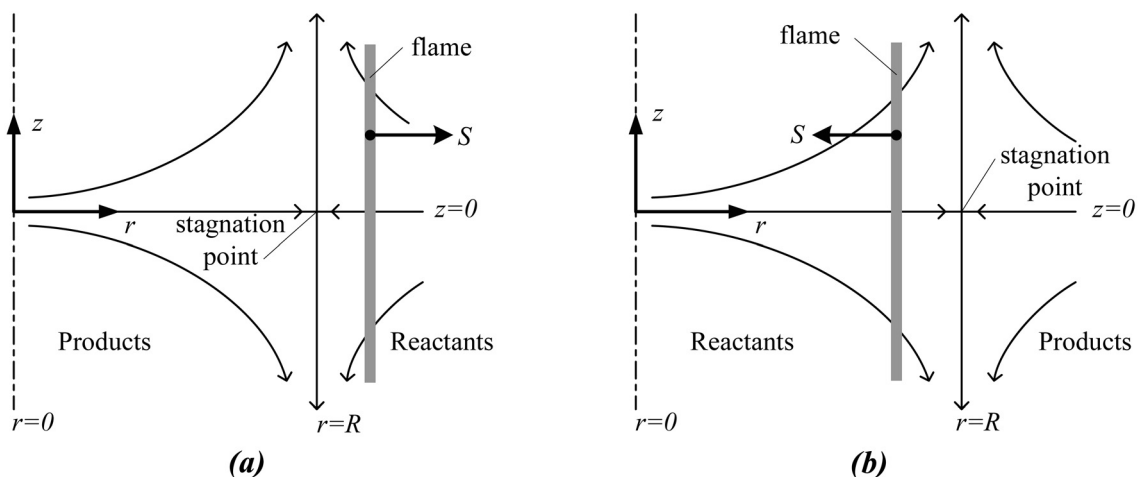


Fig. 1. Schematic representation of (a) positively curved and (b) negatively curved tubular flames in a cylindrical stagnation flow. The burning velocity  $S$  points towards the reactants.

yields the following equations for species, energy, momentum and mass conservation, respectively:

$$\rho \frac{\partial Y_k}{\partial t} + V \frac{\partial Y_k}{\partial r} = -\frac{1}{r} \frac{\partial}{\partial r} [r j_k] + \dot{\omega}_k W_k \quad (4)$$

$$\rho \frac{\partial T}{\partial t} + V \frac{\partial T}{\partial r} = \frac{1}{c_p} \left( \frac{1}{r} \frac{\partial}{\partial r} \left[ r \lambda \frac{\partial T}{\partial r} + r q_d \right] - \sum_k^K c_{p,k} j_k \frac{\partial T}{\partial r} - \sum_k^K h_k \dot{\omega}_k W_k \right) \quad (5)$$

$$\rho \frac{\partial U}{\partial t} + \rho U \frac{1}{a} \frac{da}{dt} + \rho U^2 a + V \frac{\partial U}{\partial r} = \frac{1}{r} \frac{\partial}{\partial r} \left( \mu r \frac{\partial U}{\partial r} \right) + \rho_{ub} \left( \frac{1}{a} \frac{da}{dt} + a \right) \quad (6)$$

$$\frac{\partial \rho}{\partial t} + \rho U a + \frac{1}{r} \frac{\partial}{\partial r} [r V] = 0 \quad (7)$$

where the diffusion mass flux is  $j_k = \rho Y_k V_k$  and the diffusion velocity is

$$V_k = \frac{1}{X_k \bar{W}} \sum_{j \neq k}^K \left( W_j D_{kj} \frac{\partial X_j}{\partial r} \right) - \frac{D_k^T}{\rho Y_k T} \frac{\partial T}{\partial r} \quad (8)$$

In these expressions,  $Y_k$  and  $X_k$  are respectively the mass and mole fractions of species  $k$ ;  $W_k$  and  $\dot{\omega}_k$  are the molar weight and molar production rates, respectively;  $c_p$  is the specific heat of the mixture;  $\lambda$  is the thermal conductivity;  $H_k$  is the molar enthalpy of species  $k$ ;  $\mu$  is the dynamic viscosity. The multicomponent and thermal diffusion coefficients are, respectively,  $D_{kj}$  and  $D_k^T$ . The total number of species is  $K$ .

### 2.3. Boundary conditions

The system of governing equations requires two boundary conditions each for the energy, species and momentum equations, and one boundary condition for the continuity equation. Numerical considerations require that the boundary condition at  $r = \infty$  be approximated by a boundary at a finite radius sufficiently far from the flame. The geometric dissimilarity of the boundaries at  $r = 0$  and  $r = \infty$  requires that positively and negatively curved flames be treated separately.

#### 2.3.1. Negative curvature

A natural choice for the boundary conditions is to specify the values of each variable in the unburned mixture and to set a zero-gradient condition on the products side for  $T$ ,  $Y_k$  and  $U$ . On the burned side, this choice does not work well, as the mass flux coming from the burned boundary makes the values on that boundary unresponsive to changes in the reactant boundary conditions. Instead, the temperature and composition of the burned mixture are specified. For a steady flame, this

condition is the equilibrium concentration of the chemical species at the adiabatic flame temperature. When the burned side boundary is sufficiently far from the flame, the zero-gradient condition is automatically satisfied.

The unburned boundary condition for  $U$  is by definition  $U_{ub} = 1$ . Setting the spatial derivatives in Eq. (6) to zero yields an ODE for value of  $U$  on the burned side:

$$\frac{dU_b}{dt} = -U_b^2 a - U_b \left( \frac{1}{a} \frac{da}{dt} \right) + \frac{\rho_{ub}}{\rho_b} \left( \frac{1}{a} \frac{da}{dt} + a \right) \quad (9)$$

For a steady flame, the burned-stream boundary condition on  $U$  reduces to  $U_b = \sqrt{\rho_{ub}/\rho_b}$ .

The boundary condition for the continuity equation specifies the mass flux at  $r = 0$ . While the density-weighted velocity  $V$  goes to infinity as  $r$  approaches zero, the mass flux per unit length,  $2\pi r V$ , is finite at  $r = 0$ . The boundary condition on the continuity equation is specified in terms of the corresponding non-reacting stagnation point radius  $R$ :

$$(rV)_{r=0} = \rho_{ub} \frac{a}{2} R^2 \quad (10)$$

where both  $a$  and  $R$  may be functions of time.

#### 2.3.2. Positive curvature

The boundary conditions for the positively curved flame mirror those for the negatively curved flame when the flame is sufficiently far away from  $r = 0$ . As the mass flux from the centerline is reduced and the flame radius becomes small, it becomes impossible to simultaneously specify the burned stream composition and satisfy the zero-gradient condition. However, since it was this mass flux that originally compelled the use of fixed values at the boundary, we may now once again choose to enforce the zero-gradient condition along the centerline without difficulty.

## 3. Numerical solution

The governing equations are solved numerically using a fully implicit finite difference method. A first-order backward Euler formulation is used for the time derivatives. A first-order upwind discretization is applied to all convective terms; diffusion terms are discretized to second-order using centered differences. At each time-step, all the governing equations are solved simultaneously using an inexact Newton method [8]. The linear system at each Newton step is solved using a Krylov subspace method, Bi-Conjugate Gradient Stabilized (BiCGSTAB) [9]. Further details on the numerical solution of the governing equations may be found in [3].

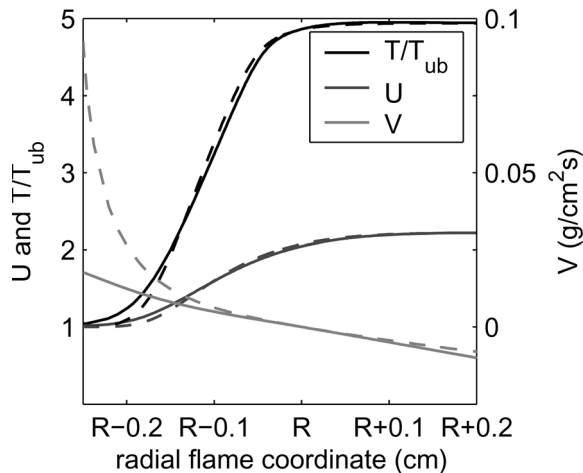


Fig. 2. Temperature ( $T$ ), mass flux ( $V$ ), and strain rate ( $U$ ) profiles in a negatively curved premixed methane-air flame;  $\phi = 0.5$ ,  $a = 100 \text{ s}^{-1}$ . Solid line corresponds to a flame with weak curvature,  $R = 10 \text{ cm}$ ; dashed line corresponds to a flame with strong curvature,  $R = 0.27 \text{ cm}$ .

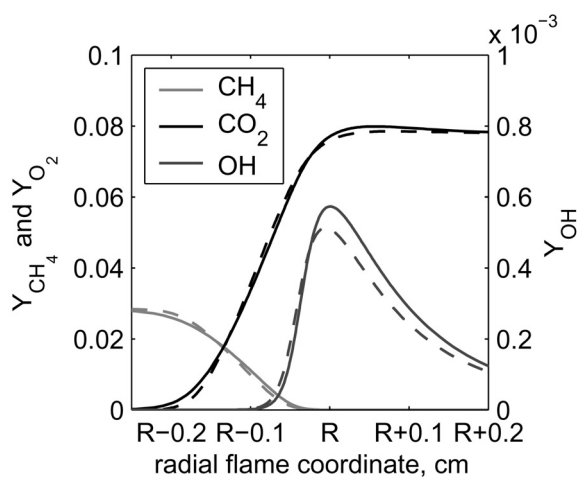


Fig. 3. Species profiles in a negatively curved premixed methane-air flame;  $\phi = 0.5$ ,  $a = 100 \text{ s}^{-1}$ . Flow and mixture conditions are identical to those in Fig. 2. Solid line corresponds to a flame with  $R = 10 \text{ cm}$ ; dashed line corresponds to a flame with  $R = 0.27 \text{ cm}$ .

Chemical source terms and mixture properties are evaluated using CHEMKIN [10]. Sandia's TRANSPORT libraries are used to evaluate the various diffusion coefficients and the mixture viscosity and thermal conductivity [11]. We use the complete GRI-Mech 3.0 kinetic model for methane-air chemistry, consisting of 325 reactions among 53 species [12].

#### 4. Results and conclusions

Figures 2 and 3 compare the structures of two negatively curved flames. Both are steady methane-air flames at a strain rate of  $a = 100 \text{ s}^{-1}$  and an equivalence ratio of  $\phi = 0.5$ ; one is weakly curved, with  $R = 10 \text{ cm}$ , and the other is more strongly curved, with  $R = 0.27 \text{ cm}$ . The impact of curvature is clearly visible on the profile of mass flux through the flame. The profiles of major species like  $\text{CH}_4$  and  $\text{CO}_2$  are only weakly influenced by curvature, while radicals like  $\text{OH}$  are more strongly affected.

In summary, we have developed an elemental flame model with detailed kinetics and transport, parameterized by an unsteady strain rate and radius of curvature. In previous studies of curved flames, strain rate and curvature were implicit properties of the model determined in post-processing. In contrast, this one-dimensional model allows the effects of curvature and strain rate to be explored independently.

Ongoing work will examine the impact of positive and negative curvature on flame structure, heat release rate, and burning velocity over a range of strain rates. We will also explore the response of the flame to unsteady strain rates and curvatures, and examine the impact of reactant mixtures containing fast-diffusing species, such as hydrogen-enhanced fuels, on the extinction properties of the flame and on the sensitivity of the flame to curvature.

#### Acknowledgments

This work was supported by the US Department of Energy, Basic Energy Sciences, MICS, under contract DE-F602-98ER25355. This research was also supported in part by an appointment to the Sandia National Laboratories Truman Fellowship in National Security Science and Engineering, sponsored by Sandia Corporation (a wholly owned subsidiary of Lockheed Martin Corporation) as Operator of Sandia National Laboratories under its US Department of Energy Contract no. DE-AC04-94AL85000.

#### References

- [1] Matalon M, Matkowsky BJ. Flames as gasdynamic discontinuities. *J Fluid Mech* 2003;124:239–259.
- [2] Chen JH, Im HG. Correlation of flame speed with stretch in turbulent premixed methane-air flames. *Proc Combust Inst* 1998;27:819–826.
- [3] Marzouk YM, Ghoniem AF, Najm HN. Towards a flame embedding model for turbulent combustion simulation. *AIAA J* 2003;41:641–652.
- [4] Im HG, Chen JH, Chen JY. Chemical response of

- methane–air diffusion flames to unsteady strain rate. *Combust Flame* 1999;118:204–212.
- [5] Echehki T, Chen JH. Unsteady strain rate and curvature effects in turbulent premixed methane–air flames. *Combust Flame* 1996;106:184–202.
- [6] Mosbacher DM, Wehrmeyer JA, Pitz RW, Sung CJ, Byrd JL. Experimental and numerical investigation of premixed tubular flames. *Proc Combust Inst* 2003;29:1479–1486.
- [7] Kee RJ, Coltrin ME, Glarborg P. *Chemically Reacting Flow: Theory and Practice*. New York: Wiley, 2003.
- [8] Pernice M, Walker HF. NITSOL: a Newton iterative solver for nonlinear systems. *SIAM J Sci Comput* 1998;19:302–318.
- [9] van der Vorst HA. Bi-CGSTAB: a fast and smoothly converging variant of Bi-CG for the solution of nonsymmetric linear systems. *SIAM J Sci Comput* 1992;13:631–644.
- [10] Kee RJ, Rupley FM, Meeks E, Miller JA. CHEMKIN-III: a Fortran chemical kinetics package for the analysis of gas-phase chemical and plasma kinetics. Technical Report SAND96-8216. Sandia National Laboratories, 1996.
- [11] Kee RJ, Dixon-Lewis G, Warnatz J, Coltrin ME, Miller JA. A Fortran computer code package for the evaluation of gas-phase multicomponent transport properties. Technical Report SAND86-8246, Sandia National Laboratories, 1986.
- [12] Smith GP, Golden DM, Frenklach M, Moriarty NW, Eiteneer B, Goldenberg M, Bowman CT, Hanson RK, Song S, Gardiner WC Jr., Lissianski VV, Qin Z. GRI-Mech 3.0. [http://www.me.berkeley.edu/gri\\_mech/](http://www.me.berkeley.edu/gri_mech/)